

## Wavelength switching by positively detuned side-mode injection in semiconductor lasers

Y. Hong and K. A. Shore<sup>a)</sup>

*School of Electronic Engineering and Computer Systems, University of Wales, Bangor, Bangor LL57 1UT, Wales, United Kingdom*

J. S. Lawrence and D. M. Kane

*School of Mathematics, Physics, Computing and Electronics, Macquarie University, Sydney, New South Wales 2109, Australia*

(Received 17 December 1999; accepted for publication 4 April 2000)

The experimental observation of a side-mode resonance regime in intermodal injection of a Fabry–Pérot semiconductor laser is reported. It is shown that wavelength switching can be easily affected by the use of positively detuned side-mode injection. Nearly degenerate four-wave mixing is observed in both positive and negative detuning regimes. © 2000 American Institute of Physics. [S0003-6951(00)02522-5]

Optical injection in semiconductor lasers has been studied extensively. Many effects of optical injection on the behavior of semiconductor lasers have been reported, such as injection locking,<sup>1</sup> four-wave mixing,<sup>2</sup> and period-doubling route to chaos.<sup>3</sup>

Much of this work is restricted to intramodal injection,<sup>1–3</sup> where the frequency  $\omega_{inj}$  of the master laser (ML) is close to the slave laser (SL) free-running frequency  $\omega_0$ . The ML frequency must be tuned within a relatively narrow bandwidth of the SL frequency. This stringent requirement on matching the frequency of the ML and SL can be relaxed by using intermodal injection locking, in which the injection is in the vicinity of a nonlasing longitudinal side mode. Goldberg, Taylor, and Weller<sup>4</sup> measured the intermodal injection locking bandwidth. Schanne *et al.*<sup>5</sup> demonstrated the existence of nearly degenerate four-wave mixing (NDFWM), where the SL side mode  $\omega_1$  became the dominant lasing mode and the coexisting side mode  $\omega_1$  and the injected beam  $\omega_{inj}$  gave rise to strong NDFWM processes and generated a conjugate beam  $\omega_2$ . Goto and co-workers<sup>6,7</sup> demonstrated intermodal injection locking using four-wave mixing. Luo and Osinski<sup>8,9</sup> have predicted that the locking bandwidth and the relaxation oscillation frequency could be enhanced under intermodal injection locking. We have recently made experimental measurements of this effect.<sup>10</sup> We also have reported bistability in intermodal injection-locked semiconductor lasers.<sup>11</sup>

In this letter, we report several regimes in intermodal injection of semiconductor lasers. The most significant regime is a side-mode resonance regime. Here, the side mode becomes the dominant lasing mode, and instead of injection locking occurring, the SL wavelength is switched from the free-running wavelength to the side-mode wavelength. We also observed that NDFWM arises in the positive detuning regime ( $\Delta\Omega = \omega_{inj} - \omega'_1 > 0$ , where  $\omega'_1$  is side-mode frequency under optical injection), as well as in the negative detuning regime ( $\Delta\Omega < 0$ ). This is similar to the case of

intramodal injection studied both experimentally and theoretically by Mogensen, Olesen, and Jacobsen.<sup>12</sup>

The experimental setup has been described previously.<sup>10</sup> The ML is a tunable laser diode (SDL-TC10-1385), with more than 20 nm tuning range. The SL is a single-mode Hitachi HLP1400 laser. Note that this laser was also used in studies reported in Refs. 5 and 12. An isolator with >60 dB attenuation is inserted between the ML and the SL to ensure that no light from the SL is injected into the ML. Two other isolators of >40 dB attenuation were used to prevent the feedback from the optical spectrum analyzer and the Fabry–Pérot interferometer used to obtain the spectral characteristics of the SL output. The SL was biased at  $\sim 1.3$  times threshold current and operated at a wavelength of 838.9 nm. The mode spacing of the SL is 0.28 nm. The wavelength difference between the free-running laser and the injection-locked state is thus 0.3 nm. It is noted that no significant change in the SL output power was observed when wavelength switching occurred. The SL free-running output power  $P_0$  is 3.05 mW. The ML lased at 839.2 nm. Injection occurs near the first side mode on the high-wavelength side of the free-running mode. During the entire experiment, the SL bias current and temperature were held constant and the free-spectrum range of the Fabry–Pérot interferometer was set at 15 GHz. The launched probe power was evaluated from the photocurrent induced in the SL at zero bias and assumed an internal quantum efficiency of 0.9. The frequency detuning is  $\Delta\omega = \omega_{inj} - \omega_1$ , where  $\omega_1$  is the side-mode frequency without optical injection. This side-mode frequency is determined by a small amount of power in it under free-running condition.

At low-injection powers, two NDFWM regimes were seen. Figure 1 shows optical spectra of the SL (using the Fabry–Pérot interferometer) with injection power ratio  $P_{inj}/P_0 = 2.4 \times 10^{-4}$ , where  $P_{inj}$  is the launched injection power. In Fig. 1(a), the detuning  $\Delta\omega$  was 3.12 GHz, where  $\Delta\Omega \approx 3.68$  GHz, the SL was lasing near the ML wavelength, and the side mode  $\omega'_1$  became the dominant lasing mode; the coexisting side mode  $\omega'_1$  and the injected beam  $\omega_{inj}$  gave rise to a strong NDFWM process and generated a conjugate

<sup>a)</sup>Electronic mail: seecs@sees.bangor.ac.uk

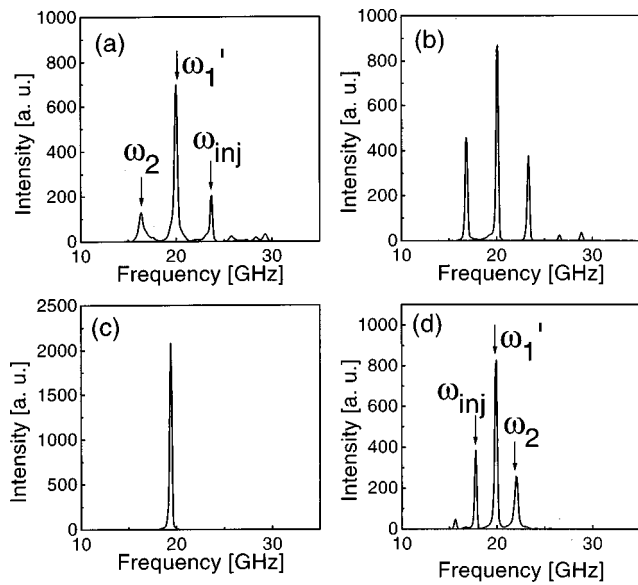


FIG. 1. Optical spectra of the SL with injection power ratio  $P_{inj}/P_0 \approx 2.4 \times 10^{-4}$ . The frequency detuning is (a)  $\Delta\omega \approx 3.12$  GHz, (b)  $\Delta\omega \approx -0.57$  GHz, (c)  $\Delta\omega \approx -1.19$  GHz, and (d)  $\Delta\omega \approx -2.96$  GHz, respectively.

beam  $\omega_2$ . When  $\Delta\omega$  was decreased, the SL wavelength changed back to the free-running wavelength: the SL was unlocked. In Fig. 1(b),  $\Delta\omega \approx -0.57$  GHz, the SL wavelength changed to the ML wavelength again. Two sidebands appear in the fine structure. These, as shown in previous work,<sup>1,10</sup> correspond to undamped relaxation oscillations. For Fig. 1(c) with  $\Delta\omega \approx -1.19$  GHz, the SL lased at the injection frequency: the SL was injection locked. Figure 1(d),  $\Delta\omega \approx -2.96$  GHz, corresponds to  $\Delta\Omega \approx -2.07$  GHz. Here the side mode  $\omega_1'$  became the dominant mode and gave rise to strong NDFWM. With further decrease of the detuning, the SL wavelength jumped back to the free-running wavelength: the SL was unlocked. It is shown that NDFWM not only appears for negative detuning, but also appears for positive detuning.

When the injection power ratio increased to  $3.76 \times 10^{-3}$ , the frequency detuning was changed; the optical spectra of the SL are shown in Fig. 2. In Fig. 2(a),  $\Delta\omega \approx 11.74$  GHz, the SL was lasing at the ML wavelength. The fine structure shows that the SL was lasing at the side-mode frequency  $\omega_1'$  (not at the injection frequency), with the main-mode intensity becoming significantly larger (here, more than 20 dB) than any other side mode. We call this the side-mode resonance. When the detuning was decreased to 8.35 GHz, the SL still lased at the ML wavelength. The optical spectrum of the SL is shown in Fig. 2(b); relaxation oscillation sidebands and harmonics appeared. As such, the laser is outside the side-mode resonance regime. For Fig. 2(c),  $\Delta\omega \approx 6.33$  GHz, the spectrum shows a broad pedestal with many broad peaks indicative of a region of chaotic dynamics. With further decreasing the detuning, many side modes appeared and the SL became unlocked. With continued decrease of the detuning, the side modes decreased, and the SL again lased at the ML wavelength, and the spectra of SL again showed evidence of chaotic dynamics. In Fig. 2(d),  $\Delta\omega \approx 2.55$  GHz, the side mode  $\omega_1'$  once more became the dominant mode and gave rise to strong NDFWM. It should be noted that the side

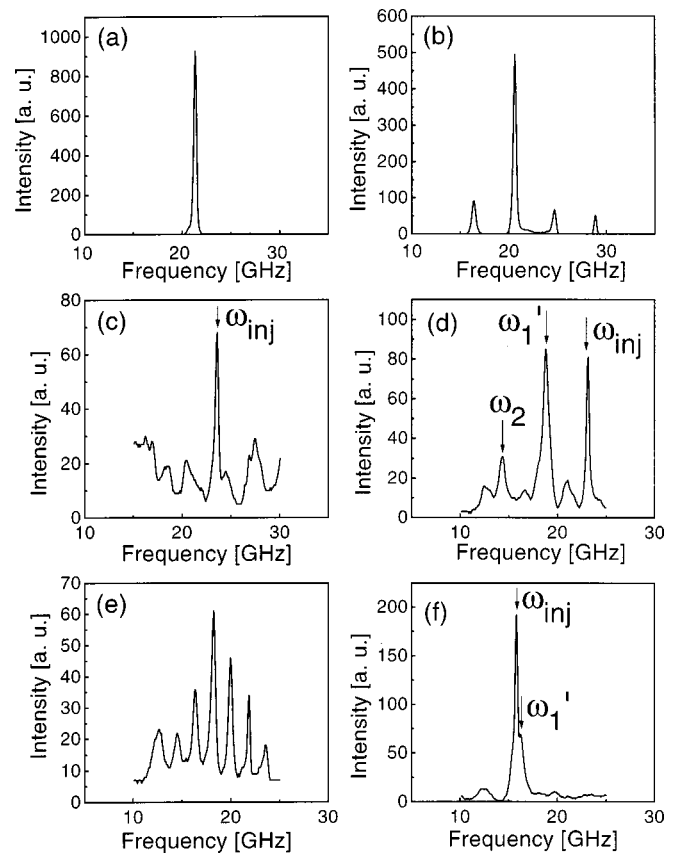


FIG. 2. Optical spectra of the SL with injection power ratio  $P_{inj}/P_0 \approx 3.76 \times 10^{-3}$ . The frequency detuning is (a)  $\Delta\omega \approx 11.74$  GHz, (b)  $\Delta\omega \approx 8.35$  GHz, (c)  $\Delta\omega \approx 6.33$  GHz, (d)  $\Delta\omega \approx 2.55$  GHz, (e)  $\Delta\omega \approx 1.26$  GHz, and (f)  $\Delta\omega \approx -4.77$  GHz, respectively.

mode under injection was shifted to a lower frequency. The frequency detuning between the injection field and side mode under injection is  $\Delta\Omega = \omega_{inj} - \omega_1' \approx 4.36$  GHz. In Fig. 2(e),  $\Delta\omega \approx 1.26$  GHz, relaxation oscillation sidebands and their harmonics or subharmonics once again appear. With further decrease of the detuning, the side mode increased and then decreased. Finally, the output power of the SL was concentrated at the ML wavelength. The optical spectra show that the SL exhibited undamped relaxation oscillations and then entered the injection-locking regime. For continued decrease of  $\Delta\omega$  to  $-4.77$  GHz, as shown in Fig. 2(f), the injection frequency is dominant, while the side-mode frequency  $\omega_1'$  appeared. As the detuning was further decreased, the SL jumped back to the free-running wavelength: the SL was unlocked. It was found that NDFWM in the negative-frequency detuning side disappears with stronger injection power.

For continued increase of the injection power ratio to  $2.74 \times 10^{-2}$ , over a large frequency detuning range (23.81 to  $-5.69$  GHz), the SL lased at the ML wavelength, while the fine structure, resolved through the Fabry-Pérot interferometer, showed that the optical spectra of the SL were quite complicated. The optical spectra of the SL show side-mode resonance, relaxation oscillation sideband and their harmonics or subharmonics, NDFWM, undamped relaxation oscillation, and injection locking at difference frequency detuning. It seems that chaotic dynamics do not exist for very high-injection power.

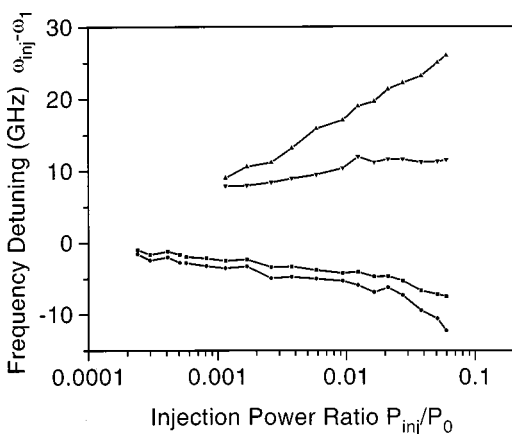


FIG. 3. Side-mode resonance and stable injection-locking regime vs injection power ratio  $P_{inj}/P_0$ . The upper and lower limits of the side-mode resonance are represented by the up and down triangles, respectively. The upper and lower limits of the stable locking range are represented by the squares and circles, respectively.

In Fig. 3 the side-mode resonance and stable injection-locking regimes at the difference injection powers are plotted. It is shown that stable injection locking is found for negative frequency detuning ( $\Delta\omega < 0$ ), as expected from theory for both intramodal and intermodal injection; the side-mode resonance arises for positive detuning ( $\Delta\omega > 0$ ). The side-mode resonance regime is much larger than the stable injection-locking regime at the high-injection level. These results imply that it is easy to switch the SL from a free-running wavelength to the side-mode wavelength when the detuning is positive. It is conjectured that the above effects arise due to a change in the gain spectrum and the differential gain during optical injection, but further careful study is required to confirm the underlying mechanism.

In summary, the dynamical behavior of a semiconductor laser under intermodal injection locking has been studied experimentally in some detail. NDFWM is observed for both positive and negative detunings for intermodal injection at low-to-medium-injection levels. As the injection level is increased, further NDFWM is observed for positive detunings only. It is known that wavelength switching can be effected by injection locking for a relatively small band of negative detuning frequencies. Here, we have discovered that for intermodal injection with positive detunings there is a significantly larger bandwidth for which wavelength switching to the side-mode frequency is easily effected. We introduce the term ‘‘side-mode resonance’’ to identify the wavelength switching found in this work.

This work was supported in part by the U.K. EPSRC under Grant No. GR/L03262.

- <sup>1</sup>I. Petitbon, P. Gallion, G. Debarge, and C. Chabran, *IEEE J. Quantum Electron.* **24**, 148 (1988).
- <sup>2</sup>H. Nakajima and R. Frey, *Phys. Rev. Lett.* **54**, 1798 (1985).
- <sup>3</sup>V. Kovanis, A. Gavrielides, T. B. Simpson, and J. M. Liu, *Appl. Phys. Lett.* **67**, 2780 (1995).
- <sup>4</sup>L. Goldberg, H. F. Taylor, and J. F. Weller, *Electron. Lett.* **20**, 809 (1984).
- <sup>5</sup>P. Schanne, H.-J. Heinrich, W. Elsässer, and E. O. Göbel, *Appl. Phys. Lett.* **61**, 2135 (1992).
- <sup>6</sup>R. Goto, T. Goto, N. Nishizawa, H. Kasuya, M. Mori, and K. Yamane, *Electron. Lett.* **34**, 2249 (1998).
- <sup>7</sup>R. Goto, N. Nishizawa, T. Goto, M. Mori, and K. Yamane, *Electron. Lett.* **35**, 1181 (1999).
- <sup>8</sup>J. M. Luo and M. Osinski, *Electron. Lett.* **27**, 1737 (1991).
- <sup>9</sup>J. M. Luo and M. Osinski, *Jpn. J. Appl. Phys., Part 2* **31**, L685 (1992).
- <sup>10</sup>Y. Hong and K. A. Shore, *IEEE J. Quantum Electron.* **35**, 1713 (1999).
- <sup>11</sup>Y. Hong and K. A. Shore, *Opt. Lett.* **23**, 1689 (1998).
- <sup>12</sup>F. Mogensen, H. Olesen, and G. Jacobsen, *IEEE J. Quantum Electron.* **QE-21**, 784 (1985).